Preparation and characterization of nanoporous resin for heavy metal removal from aqueous solution

Imed Ghiloufi, Lotfi Khezami and Lassaad El Mir

ABSTRACT

New nanoporous resin (NPR), based on organic xerogel compounds, was prepared at 150 °C by sol–gel method from pyrogallol and formaldehyde mixtures in water using perchloric acid as catalyst. NPR was characterized by scanning electron microscopy, transmission electron microscopy, X-ray diffraction and nitrogen porosimetry. The metal uptake characteristics were explored using well-established and effective parameters including pH, contact time, initial metal ion concentration and temperature. Optimum adsorptions of Cr(VI) and Cd(II) were observed at pH 3 and 4, respectively. Langmuir model gave the better fit for Cd(II) whereas for Cr(VI), Freundlich model was better than the other models to fit the experimental data. Kinetic studies revealed that the adsorption of Cd(II) was very fast compared to Cr(VI), and its data are well fitted by the pseudo-second-order kinetic model. The thermodynamic properties, i.e. ΔG°, ΔH° and ΔS°, showed that adsorption of Cr(VI) and Cd(II) onto NPR was endothermic, spontaneous and feasible in the temperature range of 27–55 °C.

Key words | adsorption, heavy metals, kinetics, nanoporous resin, thermodynamics

Imed Ghiloufi (corresponding author)
Lotfi Khezami
Lassaad El Mir
College of Sciences,
Al Imam Mohammad Ibn Saud Islamic University (IMSIU),
Riyadh,
Kingdom of Saudi Arabia
E-mail: *ghiloufimed@yahoo.fr*

Imed Ghiloufi
Lassaad El Mir
Laboratory of Physics of Materials and Nanomaterials Applied at Environment (LaPhyMNE),
Faculty of Sciences,
Gabes University,
Gabes,
Tunisia

INTRODUCTION

There are various methods for removing heavy metals from waste water including chemical precipitation, membrane filtration, ion exchange, liquid extraction or electrodialysis (Sitting 1981; Patterson 1985). These methods are not widely used due to their high cost and low feasibility for small-scale industries (Sohail *et al.* 1999). In contrast, adsorption technique is by far the most versatile and widely used. Sorbents which have been studied for adsorption of metal ions include activated carbon, fly ash, crab shell, coconut shell, zeolite, manganese oxides and resins (ion exchange and chelating).

During the past decade, several metal-retaining resins containing a variety of complexion or chelating ligands have been reported to efficiently remove heavy metals (Genc *et al.* 2002; Lebrun *et al.* 2007). Synthetic polymers containing amino, thio, oxo, carboxyl, phosphoryl and other groups have been developed. In particular, the amino/carboxyl group on an adsorbent has been found to be one of the most effective chelate functional groups for adsorption or removal of heavy metal ions from an aqueous solution (Rivas & Castro 2003; Kas goz 2006; Chen *et al.* 2007). It has also been reported that the amine groups can provide reactive sites for specific adsorption of various metal ions (Jin & Bai 2002; Li & Bai 2005; Yang *et al.* 2010).

An efficient sorbent with both high capacity and fast rate adsorption should have functional groups and large surface area (Huang *et al.* 2011). Unfortunately, most current inorganic sorbents rarely have both at the same time. On the contrary, organic polymer, polyphenylenediamine, holds a large amount of polyfunctional groups (amino and imino groups) and can effectively adsorb heavy metal ions, whereas their small specific surface area and low adsorption rate limit their application. Therefore, new sorbents with both polyfunctional groups and high surface area are still required. More recently, the development of hybrid sorbents has opened up new opportunities for their application in deep removal of heavy metals from water (Pan *et al.* 2009; Zhao *et al.* 2011). Polymer-layered silicate nanocomposites (Pavlidou & Papaspyrides 2008) have attracted both academic and industrial attention because they exhibit

doi: 10.2166/aqua.2014.086

dramatic improvement in properties at very low filler contents. The hybrid polymers were synthesized from the ring-opening polymerization of pyromellitic acid dianhydride and phenylaminomethyl trimethoxysilane (Liu *et al.* 2010).

The aim of this work is to assess the uptake of Cr(VI) and Cd(II) from aqueous solution onto nanoporous resin (NPR). In the first step, synthesis by sol–gel method of NPR is reported and structural and morphological properties investigated. In the second step, the efficiency of NPR for the adsorption of Cr(VI) and Cd(II) from aqueous solutions is studied.

MATERIALS AND METHODS

Preparation and characterization of the NPR

The preparation of NPR structure has been done in two steps. In the first one, organic xerogels were prepared by mixing formaldehyde (F) with dissolved pyrogallol (P) in water (W) solution and using perchloric acid as catalyst. The stoichiometric P/F and P/W molar ratios were 1/3 and 1/6, respectively. The wet gel was formed in a few seconds. In the second step, the obtained product was dried in a humid atmosphere at 50 °C for 2 weeks. To obtain a structured xerogel, the wet gel was transferred into an incubator and dried at 150 °C at a heating rate of 10 °C/day. The drying temperature was then maintained for 2 days, and finally the sample was cooled (El Mir *et al.* 2007). Figure 1 exhibits the reaction of the polymerization of pyrogallol and formaldehyde.

The synthesized product was characterized using a JEOL JSM-6300 scanning electron microscope (SEM) and a JEM-200CX transmission electron microscope (TEM). The specimens for TEM were prepared by putting the as-grown products in ethyl alcohol and immersing them in an ultrasonic bath for 15 min, then dropping a few drops of the resulting suspension containing the synthesized materials onto a TEM grid. The X-ray diffraction (XRD) patterns of NPR were carried out by a Bruker D5005 diffractometer, using Cu K radiation ($\lambda = 1.5418$ Å). The nitrogen adsorption–desorption isotherm of NPR was recorded by using Micrometrics ASAP2020 equipment.

Adsorption experiments

The stock solutions of cadmium and chromium were prepared by dissolving cadmium nitrate and potassium dichromate in distilled water separately. The test solutions containing single cadmium and chromium ions were prepared by diluting 1 g/L stock metal ion solution. The initial metal ion concentration ranged from 20 to 140 mg/L. The pH of each solution was adjusted to the required value with HCl or NaOH before mixing the adsorbent. Adsorption experiments were carried out in an Erlenmeyer flask by taking 10 mg of NPR in 25 mL of metal solution at the desired temperature (25 ± 1 °C) and pH. The flasks were agitated on a shaker for 12 hours, which is more than ample time for adsorption equilibrium. The amount of metal adsorbed was determined by the difference between the initial metal ion concentration and the final one after

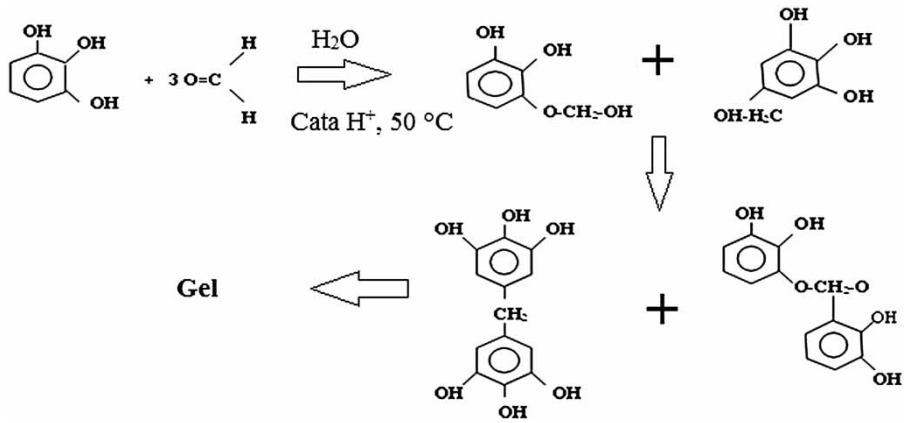

Figure 1 | Reaction of the polymerization of pyrogallol and formaldehyde.

equilibrium was reached. The residual Cd(II) and Cr(VI) concentrations were measured by SPECTRO GENESIS inductively coupled plasma-atomic emission spectrometry.

The results are given as a unit of adsorbed and unadsorbed metal ion concentration per gram of adsorbent in solution at equilibrium and are calculated by Equation (1)

$$q_e = \frac{(C_0 - C_e)V}{m} \quad (1)$$

where q_e is the adsorbed metal ion quantity per gram of adsorbent at equilibrium (mg/g), m is the weight of adsorbent (g), C_0 the initial metal concentration (mg/L), C_e the metal concentration at equilibrium (mg/L) and V is the working solution volume (L). The removal percentage was calculated by Equation (2)

$$\%\,\text{Removal} = \frac{(C_0 - C_e)}{C_0} \times 100. \quad (2)$$

RESULTS AND DISCUSSION

Adsorbent characterizations

Figure 2 exhibits the XRD patterns of the extracted product as prepared after heat drying at 150 °C in natural atmosphere. According to this diffractogram, the sample is partly amorphous, due to the presence of a small band centered at around 25°, corresponding to (0 0 2) hkl plan, the most intensive diffraction peak of crystalline graphite phase.

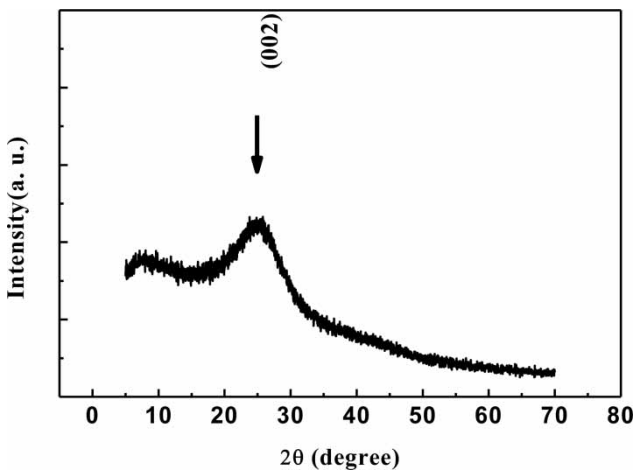

Figure 2 | XRD patterns of NPR.

The adsorption–desorption isotherm of the sample is of type I (Figure 3) in the Brunauer, Emmett and Teller (BET) classification, and characteristic of microporous solids. The microporous specific surface area is 562 m^2/g determined by the conventional BET method, with micropore volume of about 0.27 cm^3/g. The mean micropore size determined from the BET surface area and the pore volume in the approximation of cylindrical pores is close to 2 nm.

Figure 4 displays three SEM micrographs of NPR samples; particles with 1–5 μm in diameter appear to coagulate together leaving little space between them. The surface

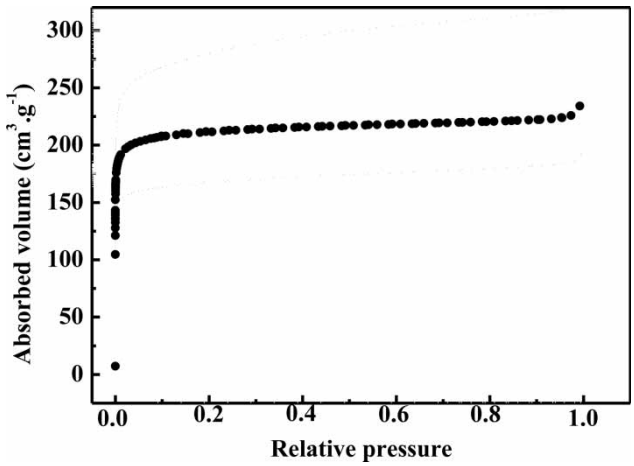

Figure 3 | Cryogenic N_2 adsorption–desorption isotherm of NPR.

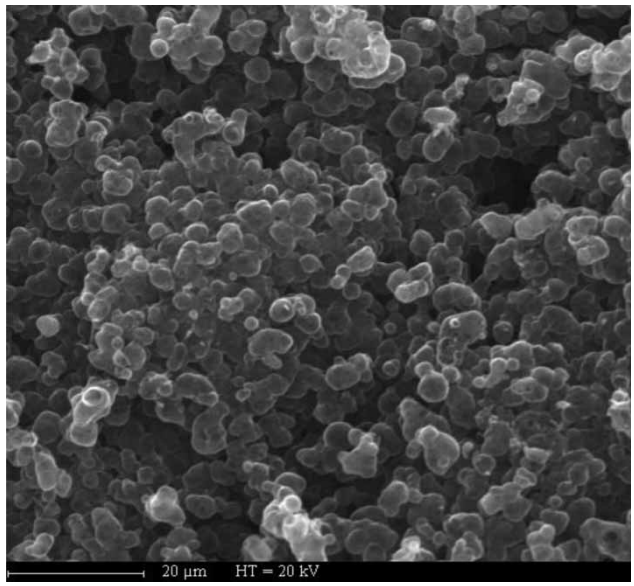

Figure 4 | SEM micrographs of NPR.

area and pore volume of this carbon indicate that these particles are essentially microporous. These results are consistent with porosity measurements.

TEM micrographs of the NPR in Figure 5 present nanospheres inside microparticles. It is clearly shown that the microparticles consist of a series of spherical nanoparticles with diameters in the range of 10 nm. These particles are arranged in a three-dimensional network. The TEM data confirm that the interconnected solid nanoparticles comprise an open-celled network with continuous nanodimension porosity. These observations are also consistent with porosity measurements.

Effect of pH

In this study the initial concentration of Cd(II) is fixed at 50 mg/L, whereas for Cr(VI) it is fixed at 45 mg/L. The mass of NPR used in this study is 10 mg. Figure 6 shows the effect of initial pH on the removal of Cd(II) and Cr(VI) using NPR. This figure shows that the cadmium adsorption by the NPR increases with increasing pH and reaches three maxima of 70.56, 68.06 and 83.175 mg/g at pH 4, pH 7 and pH 11, respectively. The low cadmium sorption at low pH value may be explained on the basis of active sites being protonated, resulting in a competition between H^+ and M^{2+} for occupancy of the binding sites (Tobin *et al.* 1984). However, for pH values between 7 and 9, lower adsorption capacity was observed; this might be due to the precipitation and lower polarity of cadmium ions at higher pH values. At pH 11 the precipitation reaction contributed to the removal of Cd(II) and the high value of q_e is not solely due to the adsorption. For this reason the pH of the solution should be lower than the critical pH of hydroxide precipitation (9.03 for Cd(II)) when considering the adsorption efficiency (Dong *et al.* 2010).

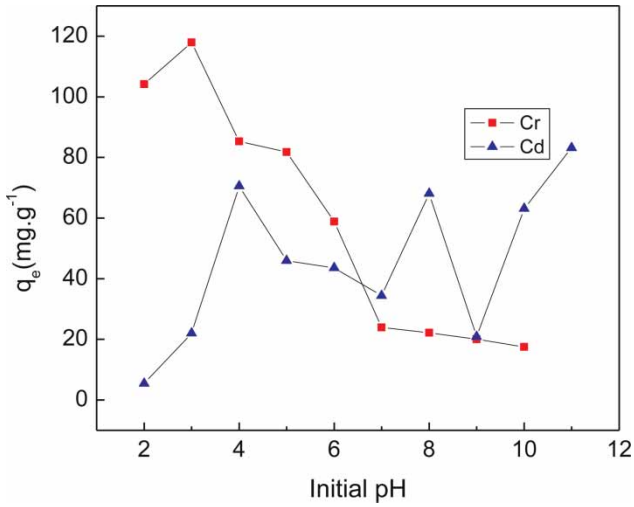

Figure 6 | Effect of initial pH on the removal of Cd(II) and Cr(VI) using NPR.

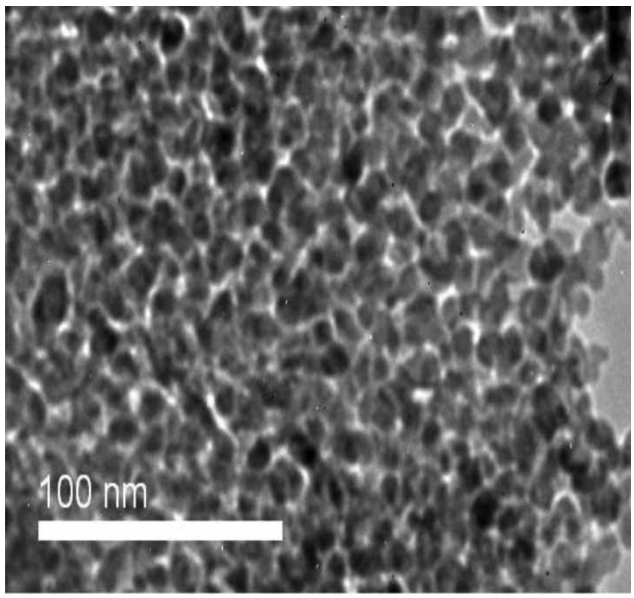

Figure 5 | TEM micrographs of NPR.

Figure 6 shows that the adsorption of Cr(VI) decreases with increase in pH from 3 to 10. The maximum removal is 117.91 mg/g and it occurred at initial pH 3. The chromate may be represented in various forms, such as H_2CrO_4, $HCrO_4^-$, CrO_4^{2-}, $Cr_2O_7^-$ and $Cr_2O_7^{2-}$ in the solution phase as a function of pH and concentration. In the pH range from 2 to 7, $HCrO_4^-$ and $Cr_2O_7^-$ are predominant. In this pH range the amounts of Cr(VI) ion can be taken by one active site of the resin in acidic condition and it is double that in alkali condition. At pH < 3, the decrease in adsorption capacity may be attributed to the competitive adsorption between Cl^- anions (Mao *et al.* 2012). For pH > 7, only CrO_4^{2-} ions exist in the solution throughout the experimental concentration range. At alkaline pH values, the sorption trend can likely be ascribed to the effect of competitive binding between CrO_4^{2-} and OH^- for the binding sites on the surface of the resins. At higher pH, an excess of OH^- can compete effectively with

CrO_4^{2-} for the bonding sites, resulting in a lower level of Cr(VI) ion uptake (Edebali & Pehlivan 2010).

Effects of contact time

In this study, 100 mg of NPR was added to each 150 mL of chromium and cadmium solutions and the pH of each solution fixed at 6.5. The initial concentrations of Cd(II) and Cr(VI) were fixed at 22.34 and 17.2 mg/L, respectively. Figure 7 shows the effect of the contact time on the sorption of Cr(VI) and Cd(II) by NPR. As can be seen from this figure, with the beginning of adsorption, the uptake of Cd(II) increased quickly, and after only 10 min the process of adsorption reached equilibrium. After this equilibrium period, the amount of adsorbed metal ions did not significantly change with time whereas for Cr(VI), the process of adsorption was very slow and reached equilibrium after 600 min.

Kinetic models

The integrated linear form of the pseudo-first-order equation can be expressed as follows (Lagergren 1998):

$$\ln (q_e - q_t) = \ln q_e - K_1 t \quad (3)$$

where q_e (mg/g) and q_t (mg/g) are the adsorption capacity at equilibrium and at time t (min), respectively, K_1 (1/min) is the rate constant of pseudo-first-order adsorption. The straight line plots of ln $(q_e - q_t)$ against t (Figure 8) were used to determine the rate constant, K_1, q_e, and correlation coefficient R^2 values of the metal ions.

The integrated linear form of the pseudo-second-order equation can be expressed as follows:

$$\frac{t}{q_t} = \frac{1}{K_2 q_e^2} + \frac{1}{q_e} t \quad (4)$$

where K_2 (g/(mg/min)) is the rate constant of pseudo-second-order adsorption. The equilibrium adsorption amount (q_e) and the pseudo-second-order rate parameters (K_2) are calculated from the slope and intercept of plot t/q_t versus t (Figure 9). Table 1 gives the kinetic parameters obtained

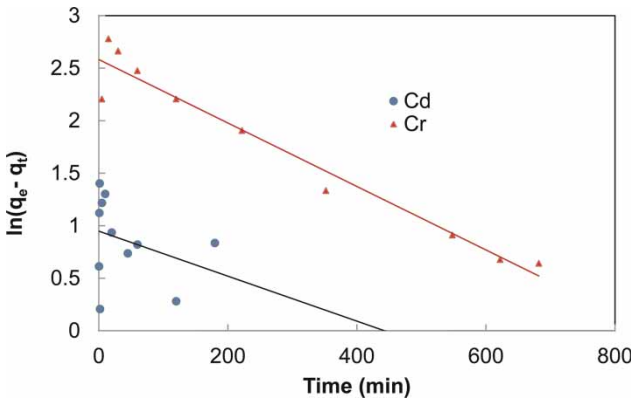

Figure 8 | Pseudo-first-order kinetic plots for Cr(VI) and Cd(II) adsorption onto NPR.

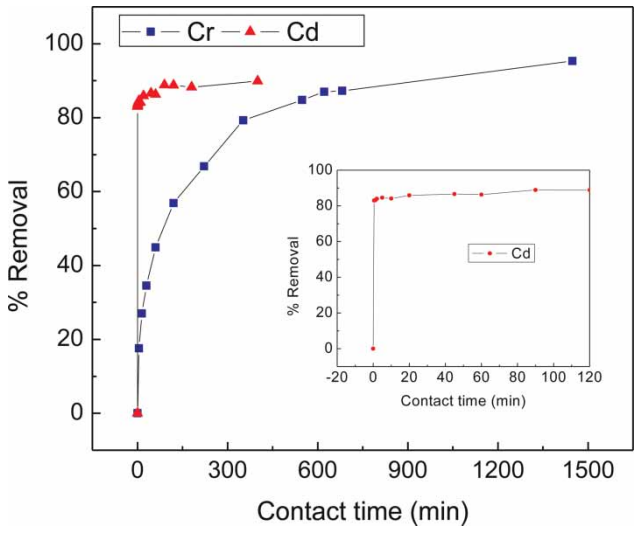

Figure 7 | Effect of contact time for Cr(VI) and Cd(II) removal onto NPR.

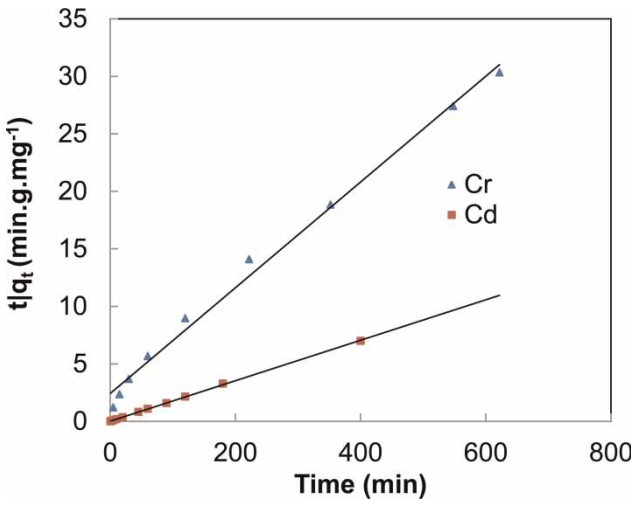

Figure 9 | Pseudo-second-order kinetic plots for Cr(VI) and Cd(II) adsorption onto NPR.

Table 1 | Adsorption kinetic model rate constants for Cd(II) and Cr(VI) adsorption on nanoporous resin

		Pseudo-first-order			Pseudo-second-order		
Ion	$q_{e,\ exp}$ (mg/g)	k_1 (1/min)	$q_{e1,\ cal}$ (mg/g)	R^2	k_2 (g/mg/min)	$q_{e2,\ cal}$ (mg/g)	R^2
Cr(VI)	22.473	3.3×10^{-3}	15.31	0.978	8.42×10^{-4}	21.93	0.994
Cd(II)	57.125	2.1×10^{-3}	2.58	0.104	1.75×10^{-2}	56.818	0.999

from pseudo-first-order and pseudo-second-order kinetic models for Cd(II) and Cr(VI) adsorption on NPR.

It can be concluded from the R^2 values in Table 1 that the sorption mechanism of Cd(II) and Cr(VI) does not follow the pseudo-first-order kinetic model. Moreover, the experimental values of $q_{e,\ exp}$ are not in good agreement with the theoretical values calculated ($q_{e1,\ cal}$) from Equation (3). Therefore, the pseudo-first-order model is not suitable for modeling the sorption of Cd(II) and Cr(VI) by NPR. However, for the pseudo-second-order, the R^2 value is 0.99 and the theoretical $q_{e2,\ cal}$ values were closer to the experimental $q_{e,\ exp}$ values (Table 1). Based on these results, it can be concluded that the pseudo-second-order kinetic model provided a good correlation for the adsorption of Cd(II) and Cr(VI) by NPR in contrast to the pseudo-first-order model.

Adsorption isotherms

Cadmium and chromium adsorption isotherms are obtained by varying the initial concentration of each metal (20–140 mg/L) at room temperature. The plot of the cadmium and chromium adsorption capacity against their equilibrium concentration is shown in Figure 10. The value of q_e increases sharply at low equilibrium concentrations whereas at higher values of C_e, the increase of q_e is slowed down.

Three models were used to fit the experimental data: Langmuir isotherm, Freundlich isotherm and Temkin isotherm.

Langmuir isotherm

The linear form of the Langmuir isotherm model is described as

$$\frac{C_e}{q_e}=\frac{1}{K_L q_m}+\frac{C_e}{q_m} \tag{5}$$

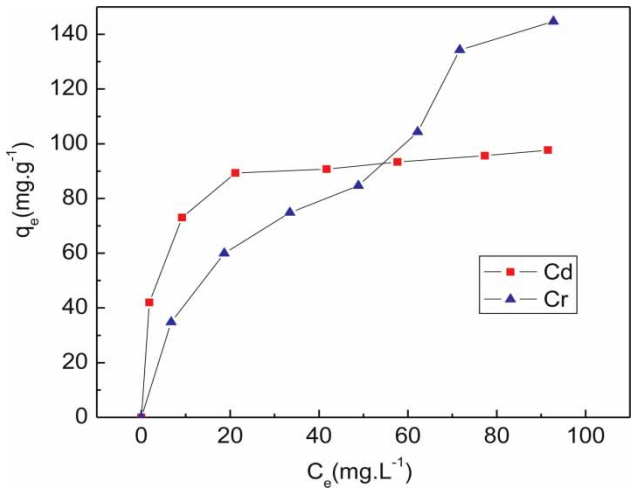

Figure 10 | Adsorption isotherm of Cr(VI) and Cd(II) by NPR.

where K_L is the Langmuir constant related to the energy of adsorption and q_m is the maximum adsorption capacity (mg/g) (Boparai *et al.* 2011). The slope and intercept of plots of C_e/q_e versus C_e were used to calculate q_m and K_L and the values of these parameters are given in Table 2.

Freundlich isotherm

The linear form of the Freundlich equation is expressed as

$$\log q_e=\log K_F+\frac{1}{n}\log C_e \tag{6}$$

where K_F and n are Freundlich isotherm constants related to adsorption capacity and adsorption intensity, respectively, and C_e is the equilibrium concentration (mg/L). The Freundlich isotherm constants K_F and n are determined from the intercept and slope of a plot of log q_e versus log C_e, and they are given in Table 2. The obtained values of n are greater than unity indicating chemisorptions (Yang 1998). Isotherms with $n>1$ are classified as L-type isotherms

Table 2 | Langmuir, Freundlich and Temkin isotherm model parameters and correlation coefficients for adsorption of Cd(II) and Cr(VI) on nanoporous resin

	Langmuir			Freundlich			Temkin		
Metal	q_m (mg/g)	K_L (L/mg)	R^2	K_F	n	R^2	b_T	K_T	R^2
Cd(II)	109.90	0.225	0.994	41.39	5	0.883	13.353	18.098	0.909
Cr(VI)	188.68	0.023	0.856	12.88	1.96	0.978	37.452	0.288	0.874

reflecting a high affinity between adsorbate and adsorbent and are indicative of chemisorptions (Yang 1998).

Temkin isotherm

The linear form of Temkin isotherm model is given by the equation

$$q_e = b_T \ln K_T + b_T \ln C_e \quad (7)$$

where b_T is the Temkin constant related to the heat of sorption (J/mol) and K_T is the Temkin isotherm constant (L/g) (Boparai *et al.* 2011). K_T and b_T were determined from the intercept and slope of a plot of q_e versus ln C_e (Table 2).

The estimated adsorption constants with corresponding correlation coefficients (R^2) are given in Table 2. For cadmium the value of correlation coefficients obtained from each model indicated that the Langmuir model is better than the Freundlich and Temkin models to fit the experimental data, which confirms that the adsorption is a monolayer, the adsorption of each molecule has an equal activation energy and the adsorbate–adsorbate interaction can be negligible. Thus, it is clear that the adsorption occurs on a homogeneous surface. The maximum adsorption capacity of Cd(II), calculated using the Langmuir model, is 109.9 mg/g at room temperature. For chromium, the correlation coefficients obtained from each model indicated that the Freundlich model was better than the Langmuir and Temkin models to fit the experimental data.

Thermodynamic parameters

The standard Gibbs free energy ΔG^o (kJ/mol) was calculated using the following equation:

$$\Delta G^\circ = -\mathrm{RT} \ln k \quad (8)$$

where k is the thermodynamic equilibrium constant, or the thermodynamic distribution coefficient, and it can be defined as

$$k = \frac{a_s}{a_e} = \frac{\gamma_s C_s}{\gamma_e C_e} \quad (9)$$

where a_e is the activity of metal ion in solution at equilibrium; a_s is the activity of adsorbed metal ion; C_s is the surface concentration of metal ion (mmol/g) in the adsorbent; C_e is the metal ion concentration in solution at equilibrium (mmol/mL); γ_e represents the activity coefficient of the metal ion in solution; and γ_s is the activity coefficient of the adsorbed metal ion. As the metal ion concentration in the solution declines to zero, k can be obtained by plotting ln (C_s/C_e) versus C_s and extrapolating C_s to zero (Chiron *et al.* 2003; Tu *et al.* 2012). The points of the obtained straight line are fitted by least-squares analysis. The intercept at the vertical axis yields the values of k. The obtained values of k and ΔG° at different temperatures are given in Table 3.

The average standard enthalpy change (ΔH°) and entropy change (ΔS°) of metal ion adsorption onto NPR were calculated by the following equation:

$$\ln K = \frac{\Delta S^\circ}{\mathrm{R}} - \frac{\Delta H^\circ}{\mathrm{RT}} \quad (10)$$

Table 3 | Thermodynamic parameters for adsorption of heavy metals on nanoporous resin

Ion	T (K)	K	ΔG° (kJ/mol)	ΔS° (J/mol/K)	ΔH° (kJ/mol)
Cd(II)	300	5.751	−4.364	53.1	1.158
	313	6.828	−4.999		
	328	8.547	−5.851		
Cr(VI)	300	1.3157	−0.684	108.4561	3.189
	313	2.1312	−1.969		
	328	3.9162	−3.722		

where ΔH° and ΔS° were calculated from the slope and the intercept in the plot of ln (k) against $1/T$, respectively. These results are shown in Figure 11. Table 3 presents the obtained values of ΔH° and ΔS° at different temperature for metal ion adsorption process on NPR.

The thermodynamic equilibrium constant k increased with temperature indicating that the adsorption was endothermic. Negative values of ΔG° for the two metal ions indicate spontaneous adsorption and the degree of spontaneity of the reaction increases with increasing temperature. The values of standard enthalpy change for Cd(II) and Cr(VI) are positive. This suggests that the adsorption of Cd(II) and Cr(VI) by NPR is endothermic, which is supported by the increasing of adsorption with temperature for the two elements. The positive standard entropy change of Cd(II) and Cr(VI) reflects the affinity of the NPR toward the two metal ions (Yang 1998).

Comparison of Cd and Cr adsorption capacity among different adsorbents

The adsorption capacity of NPR for the removal of Cd(II) and Cr(VI) has been compared to various adsorbents reported in the literature and their adsorption capacities are given in Table 4. A comparison between our work and the reported data from the literature shows that NPR is a more efficient and promising adsorbent for Cd(II) and Cr(VI) removal than other adsorbents. Therefore, it can be safely concluded that NPR has a considerable potential for the removal of Cd(II) and Cr(VI) from water and wastewater.

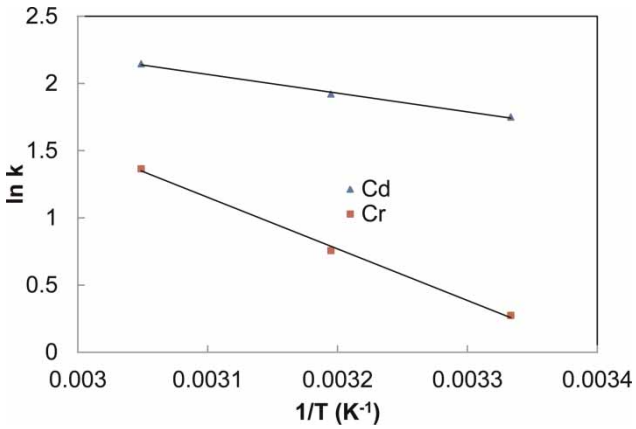

Figure 11 | Plot of ln k versus $1/T$ for the estimation of thermodynamic parameters for adsorption of Cr(VI) and Cd(II) on NPR.

Table 4 | Comparison of adsorption capacities of heavy metals for various adsorbents

Adsorbent	q_e (mg/g)	T (K)	pH	Reference
Cd(II)				
Oxidized nanoporous AC	31.4	297		Xiao & Thomas (2004)
Acid-treated AC	15.2	298	6.0	Jin *et al.* (2013)
CSTU resin	120		5	Monier & Abdel-Latif (2012)
D152 resin	378	298	5.59	Xiong & Yao (2009)
NPR	113.08	313	6.5	This work
Cr(VI)				
Amberlite IRA96 resin	33.38	298	3	Edebali & Pehlivan (2010)
Lignin-based resin (LBR)	57.68		2	Liang *et al.* (2013)
PS-EDTA magnetic resin	250	298	4	Mao *et al.* (2012)
Raw PS-EDTA resin	123.05	298	4	Mao *et al.* (2012)
KIP210 resin	102	308	3	Yang *et al.* (2014)
NPR	233.99	313	6.5	This work

CONCLUSION

Nanometer-scale resin particles with diameters in the range of 10 nm aggregated in micrometer-scale particles have been synthesized by a new protocol of sol–gel method. The NPR monolith obtained from the polymerization of pyrogallol and formaldehyde in water using perchloric acid as catalyst, presents some particular behaviors. Structural and textural analysis indicated an amorphous microporous phase with a specific surface area, micropore volume and pore size of about 562 m^2/g, 0.27 cm^3/g and 2 nm, respectively. This NPR was identified as a potential and highly efficient nanoporous structure for the removal of Cr(VI) and Cd(II) from water; the adsorption depends strongly on different parameters like pH and temperature. Kinetic studies revealed that the equilibrium was reached within 10 min for Cd(II) and within 600 min for Cr(VI) and the pseudo-second-order kinetic model provides the best correlation with the experimental data compared to the pseudo-first-order model. The maximum adsorption capacity of Cr(VI) and Cd(II) were found to be 233.99 and 113.08 mg/g,

respectively, under pH of 6.5, and temperature of 40 °C. The Langmuir model yields a better fit than the Freundlich and Temkin models for Cd(II) adsorption on NPR, whereas the Freundlich model yields a better fit than the Langmuir and Temkin models for Cr(VI) adsorption under the investigated temperatures. From the thermodynamic studies, the adsorption process was spontaneous and endothermic. These results provide the enhancement of Cr(VI) and Cd(II) uptake from aqueous solutions by NPR which is considered as adsorbent for removing metals from water and wastewater.

ACKNOWLEDGEMENT

This work was supported by the National Plan, for Sciences, Technology and Innovation, at Al-Imam Mohammed Ibn Saud Islamic University, College of Sciences, Kingdom of Saudi Arabia.

REFERENCES

Boparai, H. K., Joseph, M. & O'Carroll, D. M. 2011 Kinetics and thermodynamics of cadmium ion removal by adsorption onto nano zerovalent iron particles. *J. Hazard. Mater.* **186**, 458–465.

Chen, C. Y., Chiang, C. L. & Chen, C. R. 2007 Removal of heavy metal ions by a chelating resin containing glycine as chelating groups. *Sep. Purif. Technol.* **54**, 396–403.

Chiron, N., Guilet, R. & Deydier, E. 2003 Adsorption of Cu(II) and Pb(II) onto a grafted silica: isotherms and kinetic models. *Water Res.* **37**, 3079–3086.

Dong, L., Zhu, Z., Ma, H., Qiu, Y. & Zhao, J. 2010 Simultaneous adsorption of lead and cadmium on MnO_2-loaded resin. *J. Environ. Sci.* **22** (2), 225–229.

Edebali, S. & Pehlivan, E. 2010 Evaluation of Amberlite IRA96 and Dowex 1 × 8 ion-exchange resins for the removal of Cr (VI) from aqueous solution. *J. Chem. Eng.* **161**, 161–166.

El Mir, L., Kraiem, S., Bengagi, M., Elaloui, E., Ouderni, A. & Alaya, S. 2007 Synthesis and characterization of electrical conducting nanoporous carbon structures. *Physica B* **395**, 104–110.

Genc, O., Arpa, C., Bayramoglu, G., Arica, M. Y. & Bektas, S. 2002 Selective recovery of mercury by Procion Brown MX 5BR immobilized poly (hydroxyethylmethacrylate/chitosan) composite membranes. *Hydrometallurgy* **67**, 53–62.

Huang, M. R., Huang, S. J. & Li, X. G. 2011 Facile synthesis of polysulfoaminoanthraquinone nanosorbents for rapid removal and ultrasensitive fluorescent detection of heavy metal ions. *J. Phys. Chem. C* **115**, 5301–5315.

Jin, L. & Bai, R. B. 2002 Mechanisms of lead adsorption on chitosan/PVA hydrogel beads. *Langmuir* **18**, 9765–9770.

Jin, G. P., Zhu, X. H., Li, C. Y., Fu, Y., Guan, J. X. & Wu, X. P. 2013 Tetraoxalyl ethylenediamine melamine resin functionalized coconut active charcoal for adsorptive removal of Ni(II), Pb(II) and Cd(II) from their aqueous solution. *J. Environ. Chem. Eng.* **1**, 736–745.

Kas goz, H. 2006 New sorbent hydrogels for removal of acidic dyes and metal ions from aqueous solutions. *Polym. Bull.* **56**, 517–528.

Lagergren, S. 1998 Zur theorie der sogenannten adsorption geloster stoffe kungliga svenska vetenskapsakademiens (For the theory of so-called adsorption of dissolved substances). *Handlingar* **24**, 1–39.

Lebrun, L., Vallee, F., Alexandre, B. & Nguyen, Q. T. 2007 Preparation of chelating membranes to remove metal cations from aqueous solutions. *Desalination* **207**, 9–23.

Li, N. & Bai, R. 2005 A novel amine-shielded surface cross-linking of chitosan hydrogel beads for enhanced metal adsorption performance. *Ind. Eng. Chem. Res.* **44**, 6692–6700.

Liang, F. B., Song, Y. L., Huang, C. P., Zhang, J. & Chen, B. H. 2013 Adsorption of hexavalent chromium on a lignin-based resin: equilibrium, thermodynamics, and kinetics. *J. Environ. Chem. Eng.* **1**, 1301–1308.

Liu, J., Ma, Y., Xu, T. & Shao, G. 2010 Preparation of zwitterionic hybrid polymer and its application for the removal of heavy metal ions from water. *J. Hazard. Mater.* **178**, 1021–1029.

Mao, N., Yang, L., Zhao, G., Li, X. & Li, Y. 2012 Adsorption performance and mechanism of Cr(VI) using magnetic PS-EDTA resin from micro-polluted waters. *J. Chem. Eng.* **200–202**, 480–490.

Monier, M. & Abdel-Latif, D. A. 2012 Preparation of cross-linked magnetic chitosan-phenylthiourea resin for adsorption of Hg(II), Cd(II) and Zn(II) ions from aqueous solutions. *J. Hazard. Mater.* **209–210**, 240–249.

Pan, B., Zhang, W., Lv, L. & Zhang, Q. 2009 Development of polymeric and polymer-based hybrid adsorbents for pollutants removal from waters. *J. Chem. Eng.* **151**, 19–29.

Patterson, J. W. 1985 *Industrial Wastewater Treatment Technology*, 2nd edn. Butterworth-Heinemann, London.

Pavlidou, S. & Papaspyrides, C. D. 2008 A review on polymer-layered silicate nanocomposites. *Prog. Polym. Sci.* **33**, 1119–1198.

Rivas, B. L. & Castro, A. 2003 Preparation and adsorption properties of resins containing amine, sulfonic acid, and carboxylic acid moieties. *J. Appl. Polym. Sci.* **90**, 700–705.

Sitting, M. 1981 *Handbook of Toxic and Hazardous Chemicals*. Noyes Publications, Park Ridge, NJ.

Sohail, A., Ali, S. I., Khan, N. A. & Rao, R. A. K. 1999 Removal of chromium from wastewater by adsorption. *Environ. J. Pollut. Control* **2**, 27–31.

Tobin, J. M., Cooper, D. G. & Neufeld, R. J. 1984 Uptake of metal ions by *Rhizopus arrhizus* biomass. *Appl. Environ. Microbiol*. **47**, 821–824.

Tu, Y.-J., You, C.-F. & Chang, C.-K. 2012 Kinetics and thermodynamics of adsorption for Cd on green manufactured nano-particles. *J. Hazard. Mater*. **235–236**, 116–122.

Xiao, B. & Thomas, K. M. 2004 Competitive adsorption of aqueous metal ions on an oxidized nanoporous activated carbon. *Langmuir* **20**, 4566–4578.

Xiong, C. H. & Yao, C. P. 2009 Study on the adsorption of cadmium(II) from aqueous solution by D152 resin. *J. Hazard. Mater*. **166**, 815–820.

Yang, C. H. 1998 Statistical mechanical study on the Freundlich isotherm equation. *J. Colloid Interf. Sci*. **208**, 379–387.

Yang, L., Li, Y., Wang, L., Zhang, Y., Ma, X. & Ye, Z. 2010 Preparation and adsorption performance of a novel bipolar PS-EDTA resin in aqueous phase. *J. Hazard. Mater*. **180**, 98–105.

Yang, J., Yu, M. & Qiu, T. 2014 Adsorption thermodynamics and kinetics of Cr(VI) on KIP210 resin. *J. Ind. Eng. Chem*. **20**, 480–486.

Zhao, X., Lv, L., Pan, B., Zhang, W. & Zhang, S. 2011 Polymer-supported nanocomposites for environmental application: a review. *J. Chem. Eng*. **170**, 381–394.

First received 29 June 2014; accepted in revised form 12 October 2014. Available online 22 November 2014